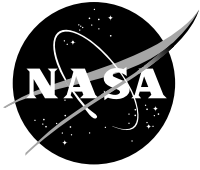


NASA/TM—2011-216808



Reliability Based Design for a Raked Wing Tip of an Airframe

Surya N. Patnaik
Ohio Aerospace Institute, Brook Park, Ohio

Shantaram S. Pai and Rula M. Coroneos
Glenn Research Center, Cleveland, Ohio

NASA STI Program . . . in Profile

Since its founding, NASA has been dedicated to the advancement of aeronautics and space science. The NASA Scientific and Technical Information (STI) program plays a key part in helping NASA maintain this important role.

The NASA STI Program operates under the auspices of the Agency Chief Information Officer. It collects, organizes, provides for archiving, and disseminates NASA's STI. The NASA STI program provides access to the NASA Aeronautics and Space Database and its public interface, the NASA Technical Reports Server, thus providing one of the largest collections of aeronautical and space science STI in the world. Results are published in both non-NASA channels and by NASA in the NASA STI Report Series, which includes the following report types:

- **TECHNICAL PUBLICATION.** Reports of completed research or a major significant phase of research that present the results of NASA programs and include extensive data or theoretical analysis. Includes compilations of significant scientific and technical data and information deemed to be of continuing reference value. NASA counterpart of peer-reviewed formal professional papers but has less stringent limitations on manuscript length and extent of graphic presentations.
- **TECHNICAL MEMORANDUM.** Scientific and technical findings that are preliminary or of specialized interest, e.g., quick release reports, working papers, and bibliographies that contain minimal annotation. Does not contain extensive analysis.
- **CONTRACTOR REPORT.** Scientific and technical findings by NASA-sponsored contractors and grantees.

- **CONFERENCE PUBLICATION.** Collected papers from scientific and technical conferences, symposia, seminars, or other meetings sponsored or cosponsored by NASA.
- **SPECIAL PUBLICATION.** Scientific, technical, or historical information from NASA programs, projects, and missions, often concerned with subjects having substantial public interest.
- **TECHNICAL TRANSLATION.** English-language translations of foreign scientific and technical material pertinent to NASA's mission.

Specialized services also include creating custom thesauri, building customized databases, organizing and publishing research results.

For more information about the NASA STI program, see the following:

- Access the NASA STI program home page at <http://www.sti.nasa.gov>
- E-mail your question via the Internet to help@sti.nasa.gov
- Fax your question to the NASA STI Help Desk at 443-757-5803
- Telephone the NASA STI Help Desk at 443-757-5802
- Write to:
NASA Center for AeroSpace Information (CASI)
7115 Standard Drive
Hanover, MD 21076-1320

NASA/TM—2011-216808



Reliability Based Design for a Raked Wing Tip of an Airframe

Surya N. Patnaik
Ohio Aerospace Institute, Brook Park, Ohio

Shantaram S. Pai and Rula M. Coroneos
Glenn Research Center, Cleveland, Ohio

National Aeronautics and
Space Administration

Glenn Research Center
Cleveland, Ohio 44135

November 2011

This work was sponsored by the Fundamental Aeronautics Program
at the NASA Glenn Research Center.

Level of Review: This material has been technically reviewed by technical management.

Available from

NASA Center for Aerospace Information
7115 Standard Drive
Hanover, MD 21076-1320

National Technical Information Service
5301 Shawnee Road
Alexandria, VA 22312

Available electronically at <http://www.sti.nasa.gov>

Reliability Based Design for a Raked Wing Tip of an Airframe

Surya N. Patnaik
Ohio Aerospace Institute
Brook Park, Ohio 44142-1068

Shantaram S. Pai and Rula M. Coroneos
National Aeronautics and Space Administration
Glenn Research Center
Cleveland Ohio 44135

Summary

A reliability-based optimization methodology has been developed to design components of an airframe structure. Design is formulated for an accepted level of risk or reliability. The design variables, weight and the constraints became functions of reliability. Uncertainties in the load, strength and the material properties, as well as the design variables, were modeled as random parameters with specified distributions, like normal, Weibull or Gumbel functions. The objective function and constraint, or a failure mode, became derived functions of the risk-level. Solution to the problem produced the optimum design with weight, variables and constraints as a function of the risk-level. Optimum weight versus reliability traced out an inverted-S shaped graph. The center of the graph corresponded to a 50 percent probability of success, or one failure in two samples. Under some assumptions, this design would be quite close to the deterministic optimum solution. The weight increased when reliability exceeded 50 percent, and decreased when the reliability was compromised. A design could be selected depending on the level of risk acceptable to a situation. The reliability-based optimization software was obtained by combining three codes. MSC/Nastran code was the deterministic analyzer. Fast probability integration of the NESSUS software was the probabilistic calculator. NASA Glenn Research Center's optimization testbed CometBoards was used as the optimizer. The optimization capability required a deterministic finite element structural model and probabilistic models for material properties, thermo-mechanical load and design variables.

Reliability-based optimization method was applied to design the raked wing tip of the Boeing 767-400 extended range airliner which is made of composite and metallic materials. The members of the wing tip were grouped to obtain a set of 13 active design variables. For constraint formulation, the structure was separated into a number of subcomponents. Strain constraints were imposed on members in the subcomponents. There were 203 strain constraints for the panels and the spars and 16 additional constraints for the rod members. Three translations and one rotation at the tip of the structure were also constrained. The design model had a total of 227 behavior constraints for two critical load cases. Constraint can be imposed on principal strain or on a failure theory for laminates. Deterministic optimum solution was generated first, followed by stochastic design. The stochastic optimization calculation required continuous running of the code for more than 5 days, but the execution was smooth and eventless. The optimum design exhibited nine active constraints consisting of eight strain and one displacement limitations. The optimization process redistributed the strain field in the structure and achieved up to a 20-percent reduction in weight over traditional design.

1.0 Introduction

The design of a structure is developed based on calculations for a given specification with the material's thermo-mechanical load, strength and Young's modulus etc. forming part of the specification. Any parameter in the specification can exhibit variation. In the traditional, or deterministic design method, the concept of a safety factor is used to accommodate this variation. For example, a 120 lbf

design load may include a safety factor of 1.5. The load, in other words, has a 40 lbf variation over a 80 lbf value that may reflect the service condition. A reliability design method, which is an alternate to the traditional deterministic concept, treats the load as a random variable with an associated distribution, for example, a normal distribution that is defined by a mean value and a standard deviation. Other parameters like strength, modulus of elasticity, weight density of material among others, become primitive random variables. Response quantities like stress, strain, displacement and frequency become derived random variables. Likewise sizing variables such as depth of a beam or thickness of a plate can be considered either as random variables or deterministic quantities. In other words stochastic optimization caters for both random and deterministic quantities.

The cumulative distribution concept can be utilized to estimate the value of a response parameter for a specified level of probability. For example, the value of stress at a particular location in a structure can be estimated to be less than or equal to 20 ksi for a 25-percent probability of success or reliability. The value can change to 30 ksi when the reliability is increased to 90 percent. Theoretically the stress value can approach infinity when there is no risk, which corresponds to one hundred percent rate of success. A design for such a situation or the most reliable structure can become extremely heavy. A plot of the weight versus reliability produces an inverted-S shaped graph. At the center of the S-graph there is a 50 percent probability of success, that is one failure in two samples. The weight increases when the reliability exceeds 50 percent. Weight decreases when the reliability is compromised. A design can be generated depending on the level of risk acceptable to a situation. For example, the landing gear of an airliner can be designed for a very high reliability, whereas it can be reduced to some extent for a raked wing tip.

Reliability-based design optimization requires a probabilistic analysis tool to predict the response for a specified reliability like one failure in N-samples. This topic is covered in Section 2.0 of this paper. The response is used to formulate the reliability-based design optimization and the problem is solved using standard optimization methodology. Reliability-based optimization, also referred to as stochastic design, is given in Section 3.0. Solutions to an academic example and an industrial strength problem are summarized in Section 4.0. The last section is devoted to concluding remarks.

2.0 Probabilistic Structural Analysis

Several probabilistic structural analysis methods are discussed in References 1 to 3. Here, the performance of four analysis methods are compared considering the example of a three bar truss shown in the Figure 1. It was observed that the response was satisfactory by all the methods. Any one of the methods can be used for design calculation. The methods compared were:

- (a) The Perturbation method (PM), (Ref. 2)
- (b) Direct Monte Carlo simulation (DMCS), (Ref. 4)
- (c) Latin hypercube simulation (LHS), (Ref. 5)
- (d) Fast probability integration of the NESSUS code (FPI), (Ref. 3)

The perturbation method has been used extensively in developing the stochastic finite element method because of its simplicity, efficiency, and versatility. The quadratic perturbation technique provides the mean value and the covariance matrix in closed form for stress and displacement, along with their sensitivities. Monte Carlo simulation is repetitive and it can be computationally expensive. The Latin Hypercube sampling technique gives comparable results to the Monte Carlo technique, but with fewer samples. For stochastic optimization calculation, the FPI analyzer is used. The FPI technique is based on a most probable point (MPP) concept. The majority of the probability is expected to be concentrated near the MPP. The MPP is located and different techniques are used to determine the probability in the failure prone region.

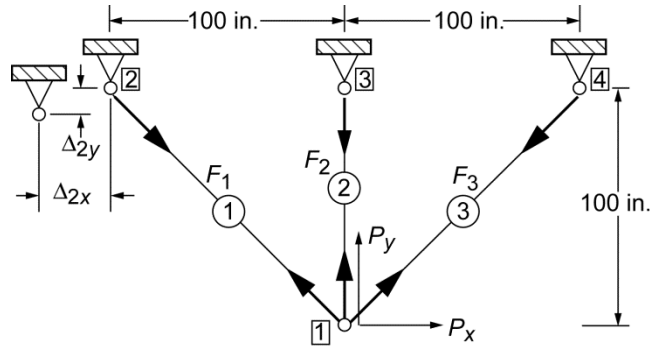


Figure 1.—Three-bar truss.

In a stochastic response analysis for a three-bar truss, as an example, the geometrical dimensions of the structure-like coordinates and bar lengths are considered deterministic in nature. The structure is subjected to mechanical load, temperature variation and settling of a support, as follows.

Mechanical load is applied at node 1 and defined by mean values and a covariance matrix as follows:

$$\text{Mean value: } \begin{Bmatrix} \mu_{P_X} \\ \mu_{P_Y} \end{Bmatrix} = \begin{Bmatrix} 50 \\ -100 \end{Bmatrix} \text{ kip and Covariance matrix: } \text{cov} \left(\begin{Bmatrix} P_X \\ P_Y \end{Bmatrix} \right) = \begin{bmatrix} 25.00 & 6.25 \\ 6.25 & 25.00 \end{bmatrix}$$

Thermal load at node 1 of the structure is subjected to a change of temperature, with a mean value of $\mu_T = 50$ °F and a standard deviation of 5 °F. The other three nodes are at ambient temperature.

The **support** at node 2 settles in both the x - and y -directions by amount $\begin{Bmatrix} \Delta_{2X} \\ \Delta_{2Y} \end{Bmatrix}$ in. as shown in Figure 1. Settling is accommodated by mean values and a covariance matrix.

$$\text{Mean value: } \begin{Bmatrix} \mu_{\Delta_{2X}} \\ \mu_{\Delta_{2Y}} \end{Bmatrix} = \begin{Bmatrix} 0.1 \\ 0.15 \end{Bmatrix} \text{ in. Covariance matrix: } \text{cov} \left(\begin{Bmatrix} \Delta_{2X} \\ \Delta_{2Y} \end{Bmatrix} \right) = \begin{bmatrix} 25.0 & 37.5 \\ 37.5 & 225.0 \end{bmatrix} \times 10^{-6}$$

The areas of the three bars (A_1 , A_2 , and A_3) are considered to be the **design variables**. Their mean values and covariance matrix are as follows:

$$\text{Mean value: } \begin{Bmatrix} \mu_{A_1} \\ \mu_{A_2} \\ \mu_{A_3} \end{Bmatrix} = \begin{Bmatrix} 1 \\ 1 \\ 2 \end{Bmatrix} \text{ in.}^2, \text{ Covariance matrix: } \text{cov} \left(\begin{Bmatrix} A_1 \\ A_2 \\ A_3 \end{Bmatrix} \right) = \begin{bmatrix} 1.00 & 0.50 & 0.25 \\ 0.50 & 1.00 & 0.25 \\ 0.25 & 0.25 & 1.00 \end{bmatrix} \times 10^{-2}$$

The 3-bar truss structure has a total of 10 primitive random variables for the material properties, loads, and sizing design parameters. The random parameters are expressed in terms of normalized primitive random variable, $\{q\}$, with zero mean, and variance given by the ratio of the standard deviation to the mean value of the corresponding stochastic variable.

$$\begin{aligned}
A_1 &= \mu_1(1 + q_1); & A_2 &= \mu_2(1 + q_2); & A_3 &= \mu_3(1 + q_3) \\
E &= \mu_4(1 + q_4); & \alpha &= \mu_5(1 + q_5) \\
P_X &= \mu_6(1 + q_6); & P_Y &= \mu_7(1 + q_7) \\
T &= \mu_8(1 + q_8); & \Delta_{2X} &= \mu_9(1 + q_9); & \Delta_{2Y} &= \mu_{10}(1 + q_{10})
\end{aligned}$$

where, (A_1, A_2, A_3) are the areas of the bars with mean values (μ_1, μ_2, μ_3) , respectively and standard deviations of $(q_1\mu_1, q_2\mu_2, q_3\mu_3)$; E is the Young's modulus with a mean value of μ_4 and a variance of (μ_4q_4) ; α is the coefficient of thermal expansion with a mean value of μ_5 and a variance of (μ_5q_5) ; (P_X, P_Y) are load values along x and y-directions with mean values (μ_6, μ_7) with variance of $(q_6\mu_6, q_7\mu_7)$; T is the temperature with a mean value of μ_8 and a variance of (μ_8q_8) ; $(\Delta_{2X}, \Delta_{2Y})$ are settling of support along x and y-directions at node 2 with mean values (μ_9, μ_{10}) and standard deviations of $(q_9\mu_9, q_{10}\mu_{10})$.

The deterministic response for forces and displacements are as follows:

$$\text{Bar forces: } \{F\} = \{\mu_F\} = \begin{Bmatrix} 62.76 \\ 61.24 \\ -7.95 \end{Bmatrix} \text{ kip and nodal displacements: } \{X\} = \{\mu_X\} = \begin{Bmatrix} 0.201 \\ -0.241 \end{Bmatrix} \text{ in.}$$

The deterministic response for forces and displacements are as follows:

$$\text{Bar forces: } \{F\} = \{\mu_F\} = \begin{Bmatrix} 62.76 \\ 61.24 \\ -7.95 \end{Bmatrix} \text{ kip and nodal displacements: } \{X\} = \{\mu_X\} = \begin{Bmatrix} 0.201 \\ -0.241 \end{Bmatrix} \text{ in.}$$

Stochastic responses were obtained using all four methods: Perturbation method, Direct Monte Carlo simulation, Latin hypercube simulation and the fast probability integration. Response for the three bar forces, stresses, and displacements by the four methods and the time to solution (CPU seconds) are depicted in Table 1. The bar forces, mean values and standard deviations were in good agreement for all four methods. The displacements showed an almost perfect match across the methods. There was a minor mismatch among the methods for bar stress. The maximum difference was about 0.8 percent in the mean value of the stress, whereas it was about 19 percent for standard deviation for the redundant member. Such a discrepancy may be confined to the redundant member with a small mean value for the parameter. Direct Monte Carlo simulation required 12,500 samples for convergence, whereas 1000 samples were sufficient for the Latin hypercube simulation. The time to calculate the response was very small, between 1 to 7 CPU seconds for both the perturbation method and the fast probability integrator. The calculation time increased significantly for the Monte Carlo and Latin hypercube simulations. The Monte Carlo simulation required about 4245 sec, which corresponded to 606 times that required by the perturbation method. Latin hypercube method took 56 times as long. Overall, the performance was satisfactory for all the methods. The Ph.D. dissertation of Wei (Ref. 2) provides merits and limitations of different probabilistic methods.

The value of the response variables for a given percent probability of success were obtained for a normal distribution function. The values of the response variables for percent probability of success ($p = 50, 25,$ and 75 percent) are listed in Table 2. A 5-percent change was seen in the forces of bars 1 and 2 between the $p = 50$ percent and $p = 75$ percent levels. For the bar 3 force, the change noted was 40 percent. A 12-percent change was seen in the horizontal displacement between the $p = 50$ percent and $p = 75$ percent levels. It was only 8 percent for the vertical displacement. In Based on these findings we conclude that the performance of all four (PM, DMC, LHS and FPI) methods is adequate.

TABLE 1.—PROBABILISTIC RESPONSE COMPARED FOR THREE-BAR TRUSS

Parameter	Perturbation method (PM)		Direct Monte Carlo simulation (DMCS)		Latin hypercube simulation (LHS)		Fast probability integrator (FPI)	
	Mean value	Standard deviation						
Force : $\begin{Bmatrix} F_1 \\ F_2 \\ F_3 \end{Bmatrix}^{\text{Kip}}$	$\begin{Bmatrix} 62.77 \\ 61.24 \\ -7.95 \end{Bmatrix}$	$\begin{Bmatrix} 4.39 \\ 4.35 \\ 4.67 \end{Bmatrix}$	$\begin{Bmatrix} 62.77 \\ 61.27 \\ -7.93 \end{Bmatrix}$	$\begin{Bmatrix} 4.39 \\ 4.35 \\ 4.67 \end{Bmatrix}$	$\begin{Bmatrix} 62.76 \\ 61.25 \\ -7.96 \end{Bmatrix}$	$\begin{Bmatrix} 4.39 \\ 4.35 \\ 4.67 \end{Bmatrix}$	$\begin{Bmatrix} 62.78 \\ 61.21 \\ -7.93 \end{Bmatrix}$	$\begin{Bmatrix} 4.39 \\ 4.35 \\ 4.67 \end{Bmatrix}$
Stress : $\begin{Bmatrix} \sigma_1 \\ \sigma_2 \\ \sigma_3 \end{Bmatrix}^{\text{Ksi}}$	$\begin{Bmatrix} 63.29 \\ 61.70 \\ -3.98 \end{Bmatrix}$	$\begin{Bmatrix} 6.71 \\ 6.20 \\ 2.34 \end{Bmatrix}$	$\begin{Bmatrix} 63.16 \\ 61.58 \\ -3.97 \end{Bmatrix}$	$\begin{Bmatrix} 5.89 \\ 5.42 \\ 2.79 \end{Bmatrix}$	$\begin{Bmatrix} 63.15 \\ 61.57 \\ -3.99 \end{Bmatrix}$	$\begin{Bmatrix} 5.77 \\ 5.38 \\ 2.75 \end{Bmatrix}$	$\begin{Bmatrix} 62.78 \\ 61.21 \\ -3.96 \end{Bmatrix}$	$\begin{Bmatrix} 6.34 \\ 6.03 \\ 2.69 \end{Bmatrix}$
Displacement : $\begin{Bmatrix} u \\ v \end{Bmatrix}^{\text{in.}}$	$\begin{Bmatrix} 0.20 \\ -0.24 \end{Bmatrix}$	$\begin{Bmatrix} 0.004 \\ 0.003 \end{Bmatrix}$	$\begin{Bmatrix} 0.20 \\ -0.24 \end{Bmatrix}$	$\begin{Bmatrix} 0.004 \\ 0.003 \end{Bmatrix}$	$\begin{Bmatrix} 0.20 \\ -0.24 \end{Bmatrix}$	$\begin{Bmatrix} 0.004 \\ 0.003 \end{Bmatrix}$	$\begin{Bmatrix} 0.20 \\ -0.24 \end{Bmatrix}$	$\begin{Bmatrix} 0.004 \\ 0.003 \end{Bmatrix}$
Computation Time								
CPU seconds	7.0		4245		390		1	
Normalized time	1.0		606		56		---	

TABLE 2.—STOCHASTIC RESPONSE FOR THREE-BAR TRUSS

Response variable	Upper limit of response variable (range) for probability of occurrence, p		
	50 percent (mean)	25 percent	75 percent
Bar force, kip			
F_1	62.76	59.80 (95%)	65.73 (105%)
F_2	61.24	58.30 (95%)	64.17 (105%)
F_3	-7.95	-4.80 (60%)	-11.09 (140%)
Displacement, in.			
u	0.201	0.178 (88%)	0.225 (112%)
v	-0.241	-0.221 (92%)	-0.261 (108%)

3.0 Stochastic Design Optimization

FPI was selected for the stochastic optimization (Ref. 3), because of the availability of the code. In stochastic optimization a design is obtained as a function of risk, or reliability p , like one failure in N number of samples. The design method accounts for uncertainties in load, material properties, failure theory and design variables. A design constraint or a failure mode is a derived function of reliability p . Solution to stochastic optimization yields the weight of a structure as a function of reliability p . When the optimum weight versus reliability p is traced an inverted-S-shaped graph results with the center of the graph corresponding to a 50 percent probability of success. A heavy design, with weight approaching infinity, could be produced for a near-zero rate of failure that corresponded to unity for reliability ($p = 1$). Weight can be reduced to a small value for the most failure-prone design with a reliability that approaches zero ($p = 0$). The stochastic optimization capability is obtained by combining three codes. The MSC/Nastran code was the deterministic analysis tool, the fast probability integration code was the probabilistic calculator and NASA Glenn Research Center’s optimization testbed CometBoards (Ref. 6) became the optimization tool. The mean value of the design parameters became the variables of the optimization problem. The standard deviation of a design variable was not altered during optimization calculations. The truss structure was designed from available bars, which had undergone reduction in the variation of the cross-sectional area along the length during the manufacturing process. In other words standard deviation in the area is a manufacturing issue and it need not be considered in the theoretical design of a truss. The weight is expressed in terms of p and the mean value of the design variables. The constraints g_j were derived from random response variables within prescribed random upper and lower

bounds g_j^U and g_j^L , respectively, with a specified percent probability (p between 0 and 1), as: $(g_j^L \leq g_j \leq g_j^U) \geq p$. A typical stochastic constraint (for stress limitation $\tau \leq \tau_0$) has the following form:

$$g_j(p) = \left[\frac{\mu_{\tau_1}}{\mu_{\tau_{10}}} - 1 \right] + \left[\Phi^*(p) \frac{\sqrt{\sigma_{\tau_1}^2 + \sigma_{\tau_{10}}^2}}{\mu_{\tau_{10}}} \right] \leq 0 \quad (1)$$

where, p is reliability, μ_{τ_1} is the mean value of stress, μ_{τ_0} is the allowable stress, Φ^* is the critical phi parameter, σ_{τ_1} is the standard deviation of stress and σ_{τ_0} is the standard deviation of stress allowable. The resulting optimization problem was solved using the optimization code CometBoards.

4.0 Numerical Examples

The stochastic design optimization capability is illustrated considering two examples:

(1) A tapered beam. The deterministic and stochastic design concepts are compared through this example. The solution is amenable to a verification by an interested reader.

(2) The composite raked wingtip of Boeing 767–400 extended range airliner. Solution was generated for the complicated design problem using stochastic design optimization methodology.

4.1 A Tapered Beam

The beam was made of aluminum with Young’s modulus $E = 10,000$ ksi and weight density $\rho = 0.1$ lb/in.³. It had a length of $2a = 144$ in. The depths (d_1, d_2) were the two design variables, as shown in Figure 2. The uniform thickness of the beam was set to $t =$ in. The beam was subjected to a transverse load $P = 20$ kip at the tip. The allowable stress limit was $\sigma_0 = 20$ ksi and tip displacement was not to exceed 1 in. ($\delta \leq 1$).

For stochastic optimization, a normal distribution was considered for the primitive random variables with a mean value (μ) and a standard deviation ($\bar{\sigma}$). The numerical values for the mean value and the standard deviation for the primitive variables are listed in Table 3. The values in the table were assumed, not measured quantities. Inaccuracy in the primitive variables could propagate into stochastic design, which became the primary limitation of the method. The design calculations used MSC/Nastran for deterministic analysis, FPI was the probabilistic estimator while CometBoards was the optimizer.

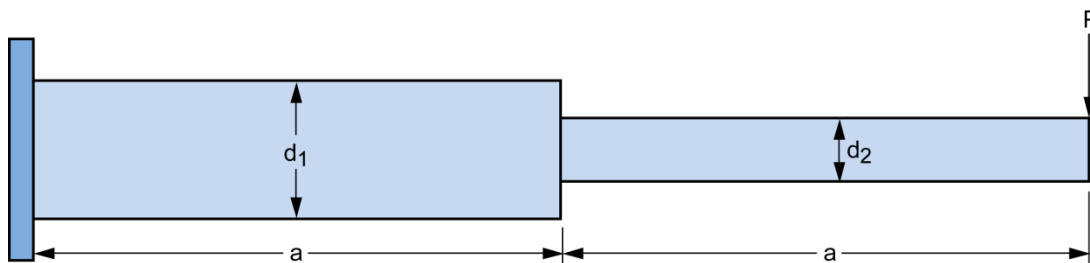


Figure 2.—Tapered beam.

TABLE 3.—MEAN VALUE AND STANDARD DEVIATION
FOR PRIMITIVE VARIABLES FOR TAPERED BEAM

Primitive variable	Mean value	Standard deviation
Stress limit: σ_0	$\mu_{\sigma_0} = 25$ ksi	$\bar{\sigma}_{\sigma_0} = 2.5$ ksi
Disp. limit: δ	$\mu_{\delta} = 1.25$ in.	$\bar{\sigma}_{\delta} = 0.125$ in.
Modulus: E	$\mu_E = 10,000$ ksi	$\bar{\sigma}_E = 1,000$ ksi
Density: ρ	$\mu_{\rho} = 0.1$	$\bar{\sigma}_{\rho} = 0.005$ in.
Load: P	$\mu_P = 15$ kip	$\bar{\sigma}_P = 3$ kip
Depth:	$\mu_{d_1} = 25$ in. and $\mu_{d_2} = 10$ in.	$\bar{\sigma}_{d_1} = 3$ in. and $\bar{\sigma}_{d_2} = 2$ in.

4.1.1 Deterministic Design for Tapered Beam

For strength constraints only the design is obtained using the flexure formula because it is a determinate structure. (Design^{strength}: $d_1 = 14.7$ in., $d_2 = 10.4$ in., weight = 722.9 lbf, $\delta = 2.31$ in.). The design is not feasible because the displacement of 2.31 in. is more than the allowable established at 1.0 in. It may not be straightforward to generate a feasible design with least weight using a traditional method even for the trivial problem.

The problem has a closed form solution for the displacement function (δ_{tip}) as follows:

$$\delta_{tip} = \frac{Pa^3}{E} \left(\frac{7}{d_1^3} + \frac{1}{d_2^3} \right) \quad (2)$$

Designs generated by several different methods are listed in Table 4. The first three methods in the table, that did not use optimization technique produced displacement as the active constraint, but the weight was not a minimum. An active condition for the displacement constraint given by Equation (2), allows the determination of a pair (d_1 and d_2) for which the weight ($w_{d_1 d_2}$) can be back calculated. In principle there are an infinite sets of (d_1 and d_2) and ($w_{d_1 d_2}$) but only one set is believed to produce the minimum condition for the weight and this can be achieved by a mathematical programming technique of operations research. Minimum weight condition cannot be calculated otherwise. The minimum weight was obtained by the optimality criteria method. Design solutions generated by the quadratic programming method (NLPQ) and the cascade strategy (Ref. 7) produced near optimal solutions, as shown in Table 4. For the purpose of reference, the stochastic design solution for rate of one failure in twenty samples as well as one in a million samples are also listed in the table. The design for ($p = 0.05$) with a weight of 949.7 lbf was quite close to the deterministic optimum solution. A very reliable design was twenty five percent heavier.

TABLE 4.—DESIGN OF TAPERED BEAM BY DIFFERENT METHODS

Method	Design variables (in.)		Weight (lbf)	Max stress (ksi)	Max disp (in.)
	d_1	d_2			
Simple proration	19.4	13.8	955.6	11.4	1.0
Engineering	25.0	10.4	1018.1	20.0	1.0
Weighted proration	25.5	10.4	1034.1	20.0	0.98
Optimality criteria	20.4	12.5	946.9	13.8	1.0
NLPQ	20.4	12.6	951.9	13.6	1.0
Cascade strategy	20.5	12.5	951.9	13.8	1.0
Stochastic design for 1 failure in 20 samples	20.2	12.5	949.7	----	----
Stochastic design for 1 failure in 1,000,000 samples	25.3	15.6	1178.0	----	----

4.1.2 Stochastic Design for Tapered Beam

Stochastic design solutions were obtained for the tapered beam for failure rate ranging from one-failure in two-samples to one-failure in 2,000,000 samples. The solutions are listed in Table 5. The optimum weight varied from 802 lbf for a 50 percent chance of survivability to 1189.0 lbf for a very reliable design. Displacement constraint was active for each design case. The weight versus reliability data is shown in Figure 3. The x-axis, representing reliability was in the range of least reliable (or 2,000,000 failures in 2,000,001 samples) to most reliable (or one failure in 2,000,000 samples). The range for the weight was from 387.3 to 1189.0 lbf. Its centroid of the inverted S-shape line corresponded to a design with a weight of 802 lbf with a 50 percent rate of survival. The graph is anti-symmetrical about its centroid. The most reliable design with a rate of one failure in 2,000,000 samples has a weight of 1191 lbf which is about 50 percent heavier than the mean valued design.

TABLE 5.—STOCHASTIC DESIGN FOR TAPERED BEAM

N (One failure in N samples)	Design variable d_1 (in.)	Variable d_2	Weight in lbf (mean value)
2	17.2	10.6	801.7
10	19.8	12.2	921.0 (947 for deterministic solution, see Table 4)
100	21.5	13.2	1000.5
1000	22.7	14.0	1055.4
10,000	23.6	14.6	1100.6
100,000	24.5	15.1	1140.6
200,000	24.7	15.2	1152.1
500,000	25.1	15.4	1167.0
1,000,000	25.3	15.6	1178.0
1,250,000	25.4	15.6	1181.6
2,000,000	25.5	15.7	1189.0

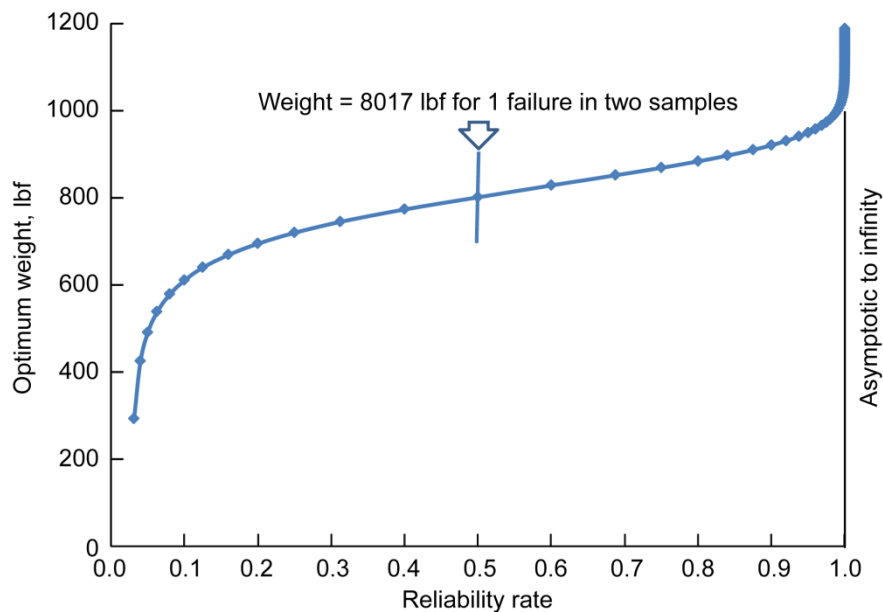


Figure 3.—Inverted-S-shaped graph for the tapered beam.

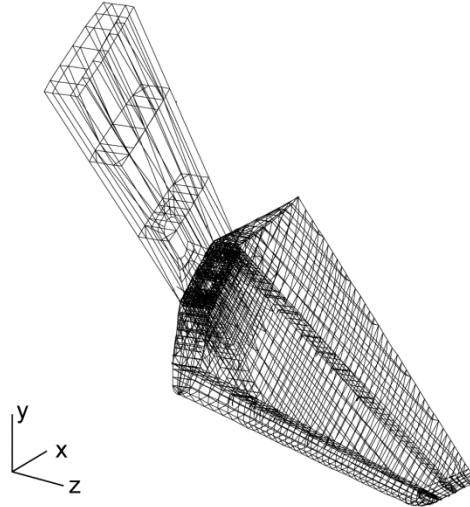


Figure 4.—Model of raked wing tip of Boeing B-767-400 extended range airliner.

4.2 Raked Wingtip Structure

A reliability-based optimum design was calculated for a composite airframe component of the Boeing 767-400 extended range airliner, also referred to as the raked wingtip structure, as shown in Figure 4. The structure was fabricated out of component parts made of metallic and composite materials. The available industrial design was referred to as the initial design. A deterministic solution and a stochastic design were generated for the component. The structure had a typical wing-box type of construction with face sheets and web panels made of composites laminates with an aluminum honeycomb core. The finite element model had about 3000 nodes and 17,000 degrees of freedom. The model was made of 3500 elements, consisting of CBAR, CBUSH, CELAS1, CHEXA, CONROD, CPENTA, CQUAD4, CROD, CSHEAR, and CTRIA3 elements of MSC/Nastran code. The structure was subjected to eight load cases. The overall response of the initial design for the eight load cases is depicted in Table 6.

TABLE 6.—RESPONSE OF THE COMPOSITE RAKED WING TIP.

Load case	Strain energy, U (in.-kip)	Maximum displacement (in.)	Maximum von Mises stress for metal (ksi)	Maximum principal microstrain in composite plies
1	9.3	-5.63	38.2	2427
2	39.8	11.56	67.4	5450
3	34.4	10.59	65.7	4920
4	33.0	10.36	66.1	4940
5	8.9	-5.54	35.5	2600
6	54	13.68	87.7	7470
7	44.3	12.45	84.8	6980
8	28.2	10.60	61.6	4180

Frequency for first three modes: 12.69, 16.34 (cantilever mode), and 17.07 Hz.

The strain energy U in the first column in Table 6 was obtained as one-half of the product of load P and displacement X over all nodes using the following formula:

$$U = \left(\frac{1}{2}\right) \int_{\text{Volume}} (\text{strain} \times \text{stress}) dv = \frac{1}{2} \left(\sum_{j=1}^{\text{all nodes and directions}} P_j X_j \right) \quad (3)$$

The strain energies for the eight load cases were in the range 9 to 54 in.-kip. Load case 6 contained the peak value for strain energy of 54 in.-kip. The maximum displacement for the load case was 13.68 in. Maximum strain in the composite components was 7470 microstrain. The maximum stress in metals was 87.7 ksi. The structure was designed for the critical load case 6 and checked against other load cases. The proposition to design for a load case with maximum strain energy drastically reduced the number of calculations during the design optimization, and it was subsequently proved to be the correct approach for the problem. The first three frequencies were in the (12.5 to 17.0) Hz range and the middle frequency of 16 Hz corresponded to a cantilever mode.

4.2.1 Deterministic Optimization for the Raked Wingtip Structure

The objective of the optimization study was to reduce the weight of the wingtip structure without changing its geometrical configuration. Only the thicknesses of the laminates were allowed to be adjusted within prescribed bounds. For design optimization the raked wingtip was separated into several substructures made of metallic and composite materials. From a preliminary design optimization study it was concluded that the thickness of titanium components and aluminum parts like, root rib center section, leading and trailing edge webs, as well as leading edge and tip rib skins cannot be changed from a manufacturing consideration. Design variables associated with these parts were considered passive. The remaining members were grouped to obtain a total of 13 design variables. The first design variable represented a thickness parameter for a total of 211 CQUAD4 and CTRIA3 elements. Likewise, the design variable 10 represented the area parameter for spars. Other design variables were defined in a similar manner. For constraint formulation, the structure was separated into 203 groups of elements to obtain a total of 203 strain constraints. The rod elements were grouped to obtain 16 more strain constraints. Three translations and one rotation were constrained at a tip node of the structure for load case 6 as well as for load case 7 to obtain eight displacement constraints. The design model had a total of 227 behavior constraints. Constraint can be imposed on principal strain, or using a failure theory, or on a strain component. The allowable strain was 4000 microstrain. Displacement limitations along x -, y -, and z -directions were set at 0.5, 1.5, and 14 in., respectively. Maximum rotation was not to exceed 5°. Design optimization was performed using the testbed CometBoards. Deterministic optimum solution is given in Table 7. Only a normalized optimum solution could be given because of the proprietary nature of the data.

Stress and strain obtained from the finite element model were presumed not to be accurate at some locations. Such localized regions were avoided in design calculations by excluding the associated strain constraints. In Table 7 column 2, model 1, referred to a configuration that was obtained by excluding the strain constraints for a set of interface elements. Likewise model 2 excluded strain constraints associated with another set of elements.

Optimum weight for model 1 was 16 percent lighter than that of the original design, or the normalized weight of 100 unit for the original design was reduced to 84 unit. The weight saving was 20 percent for model 2. Design changed throughout the structure except for variables 12 and 13, which represented the minimum thicknesses. Maximum reduction was observed for design variable 8 with a 44 percent change. The thickness reduced to 0.44 in. if the original value was 1 in. In other words, in the original structure the entire region that was associated with design variable 8 which represented an overdesigned condition. The thickness variable 6 for model 1 increased to 1.24 in. from its assumed value of 1 in., indicating a region which was under designed in the original structure. The design process redistributed the strain field with many active constraints. There was little change in the displacement state or frequency value for model 1. For model 2, maximum displacement was reduced by 2.5 percent, but its frequency increased by 25 percent because of a 20 percent reduction in its weight. Generation of a deterministic optimum solution for model 1 required about 39 CPU minutes.

TABLE VII.—NORMALIZED DETERMINISTIC OPTIMUM SOLUTION

	Original design	Design model 1	Design model 2
Weight →	100 units*	84.0 units	80.0 units
Design variables	Normalized to unity	Change in percent (100 represents no change)	
1	1.0	70.1	70.1
2	1.0	104.5	99.83
3	1.0	110.3	111.83
4	1.0	75.64	76.97
5	1.0	44.85	44.45
6	1.0	123.35	80.96
7	1.0	84.17	94.45
8	1.0	44.08	44.88
9	1.0	86.12	83.59
10	1.0	88.09	88.09
11	1.0	73.83	73.83
12	1.0	100.00	100.00
13	1.0	100.00	100.00
Active strain constraints	-----	6 with 4000 microstrain; 9 exceeded 3600 microstrain	6 with 4000 microstrain; 9 exceeded 3600 microstrain
Displacement in z-direction, in. (limit was 14 in.)	13.68	13.14	13.35
Rotation, deg (limit was 5°)	4.24	4.48	4.72
Frequency, Hz	16.36	16.45	20.33

*Normalized to 100 units.

4.2.2 Probabilistic Analysis for the Raked Wingtip Structure

For probabilistic analysis all design variables of the deterministic optimization solution were considered to be random variables. Their mean values were equal to the deterministic optimum solutions. Their standard deviations were set at 7.5 percent of the mean values. The thicknesses of the honeycomb were considered as random variables. Their mean values were equal to that of the initial design with a standard deviation of ten percent of the mean values. Cross-sectional areas of the bars were considered to be deterministic parameters and were equal to the optimum solutions. Each load component is considered to be a random variable with a mean value equal to 66.67 percent of the deterministic value with a 10-percent standard deviation. For example, if a deterministic load component is 100 lbf, then its random counterpart would have 66.67 lbf for its mean value with 6.67 lbf standard deviation. Each load component was changed in a similar manner. This refers to load model A. A second load, model B, was generated following the procedure for load model A but with a reduced mean value of 50 percent of the deterministic value. A standard deviation was set at 10 percent of the mean load value. The modulus of elasticity as well as Poisson’s ratio were considered as random variables. The standard deviations for all the material parameters were set at 7.5 percent of their mean values. The mean values were set to 105 percent of their deterministic values for the Young’s modulus and shear modulus of fabric as well as the shear modulus for the honeycomb. The mean value for Poisson’s ratio was selected to be 100 percent of its deterministic value.

The probabilistic solution was obtained using the MSC/Nastran code and the FPI software. Four different types of distributions were considered: normal, Weibull function, Lognormal, and Gumbel type 1 distributions. The probabilistic analysis produced the mean value of strain (in a certain element number 11531) to be 5050 microstrain by all four types of distribution functions (see row 1 in Table 8). Likewise, the standard deviation remained the same at 16 percent of the mean value by all four distribution functions. The mean value of displacement (at a certain node 11243 in the z-direction) was 9.6 in. with a standard deviation of 10 percent by all four distributions. The observation that the mean values and standard deviations did not change for different distribution types was as expected.

TABLE 8.—PROBABILISTIC RESPONSE FOR DIFFERENT PROBABILITY LEVELS*

N samples	Microstrain in element 11531				Displacement at node 11243 along z-direction			
	Normal	Weibull	Lognormal	Gumbel type 1	Normal	Weibull	Lognormal	Gumbel type 1
Mean value	5050	5050	5050	5050	9.7	9.7	9.7	9.7
Standard deviation	810	810	810	810	0.98	0.98	0.98	0.98
2	5050	5123	4986	4917	9.7	9.7	9.6	9.4
1,000	7555	6967	8162	9050	12.6	11.7	13.1	14.4
50,000	8379	7398	9599	11523	13.6	12.2	14.5	17.4
100,000	8507	7459	9843	11961	13.7	12.2	14.7	17.9
500,000	8903	7591	10402	12977	14.1	12.3	15.2	19.1
1,000,000	9264	7644	10641	13415	14.2	12.4	15.5	19.7
10,000,000	9264	7804	11424	14870	14.7	12.6	16.2	21.4

*The first and second rows provide the mean values and standard deviations. Remaining data in Table 7 represent mean values.

Probabilistic solution for the strain and the displacement for all four distributions of different failure rates is given in Table 8. For a 50-percent probability of failure, or one failure in two samples, the mean value and the calculated strain are equal at 5050 microstrain for normal distribution. Consider one failure in 1,000,000 samples. The Weibull prediction was conservative. It was about 85 percent of the normal distribution for strain as well as displacement. Estimates by the Gumbel type 1 distribution was on the higher side. For one failure in a million samples, it predicted about 40 to 45 percent higher strain and displacement than that for the normal distribution function.

4.2.3 Stochastic Design Optimization for Wingtip Structure

Stochastic optimization was performed for the two deterministic design models, model 1 and model 2 as discussed earlier (see Table 7). The probabilistic design calculation used the information given for stochastic analysis along with additional data required to formulate failure modes or the design constraints. It was assumed that mean value of allowable strain was 25 percent higher than its deterministic limit, while the standard deviation was set at 7.5 percent of the mean value. For example, the limits for strain were set with a mean value of 5000 microstrain and a standard deviation of 375. From deterministic optimization calculations, it was observed that only the displacement limitation along the z-direction and rotation had some influence in the design while other stiffness constraints were quite passive. Thus, for probabilistic design only two stiffness constraints were retained. At the tip (node 11243, along the z-direction), the mean value and standard deviation for the displacement limit were 17.1 and 1.71 in., respectively. The mean value and standard deviation for rotation limit were set at 6.25° and 0.625°, respectively. For the design calculation normal distributions were assumed for all random parameters. The optimization calculation required over 5 days of continuous running of the code, but the execution was smooth and eventless. The stochastic optimum solution was quite similar to that obtained for deterministic calculation. There were numerous active strain, displacement, and rotation constraints. The normalized optimum weight obtained for different failure rates is given in Table 9. The weight increased as risk was decreased. The normalized optimum weight was set to 100 for strength and stiffness constraints for load case A in design model 1 for 1 failure in 2,000,000 samples. This design exhibited nine active constraints consisting of eight strain and one displacement limitation. The frequency was 15.94 Hz for the optimum solution. One stochastic design optimization run with 61 *p* levels required 128 hr, or 5.33 days.

TABLE 9.—PROBABILITY OF FAILURE VERSUS WEIGHT

N samples	Normalized optimum weight			
	Design model 1 and load model A (strength + stiffness)	Design model 1 and load model A (strength only)	Design model 1 and load model B [strength or (strength + stiffness)]	Design model 2 and load model A (strength + stiffness)
2	64.68	64.68	62.24	63.20
10	67.43	67.43	63.57	64.36
100	70.47	70.47	65.51	66.97
1000	73.75	73.75	66.97	69.57
10,000	76.64	76.64	68.23	72.48
100,000	79.28	79.03	69.70	76.25
1,000,000	92.93	82.27	71.57	91.21
1,250,000	94.88	82.55	71.76	93.41
2,000,000	100.00	83.15	72.16	98.60

4.2.4 The Inverted S-Shaped Graph for the Wingtip Structure

The weight versus probability of success given in Table 9 was plotted in a log scale (log(N)) along the x-axis, as shown in Figure 5. This graph represented one-half of the inverted-S graph because probability of success less than 50 percent was not included. This graph was for load case A, design model 1; both strength and stiffness constraints were considered, and column 2 in Table 9 contained the weight information. The figure could be approximated into two linear segments. At the intersection point (SD) both strength and stiffness constraints were active. From the origin to the point SD, only strength constraints were active. From point SD onwards, both strain and stiffness constraints are active.

The variation of weight shown in Table 9 was expected. The weight was least for a 50-percent rate of success, or for N = 2. The weight increased when failure rate or risk was reduced. The weight in the second and third columns in the Table 9 coincided up to 1 failure in 10 000 samples because only strength constraints were active. The weight increased when both strength and stiffness constraints became active. Weight shown in column 4 was lighter than that in column 2 because load model B was less severe than load model A. Weight shown in column 5 was lighter than that in column 2 because design model 2 was obtained by removing a few severely strained constraints from model 1.

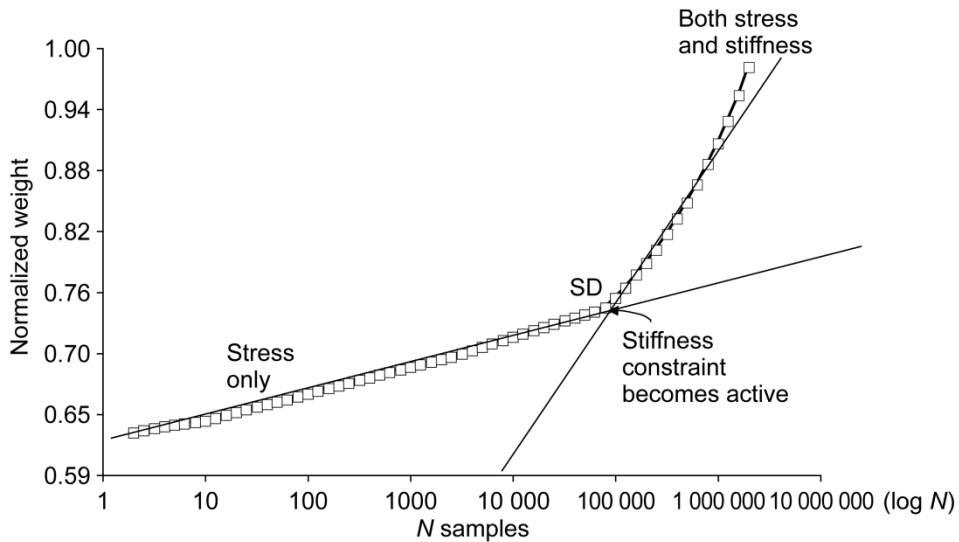


Figure 5.—Inverted-S graph in log scale for design model 1 and load case A.

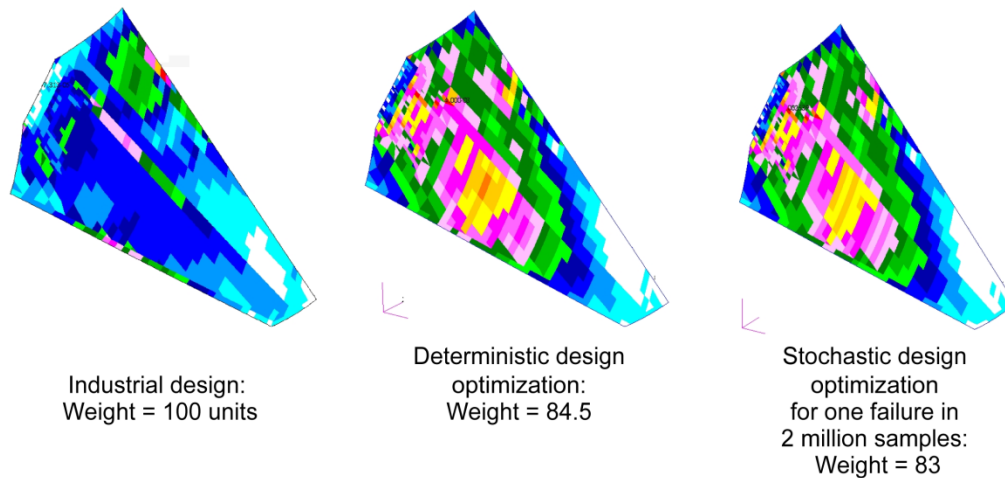


Figure 6.—Optimization process more evenly distributed the strain field in wingtip.

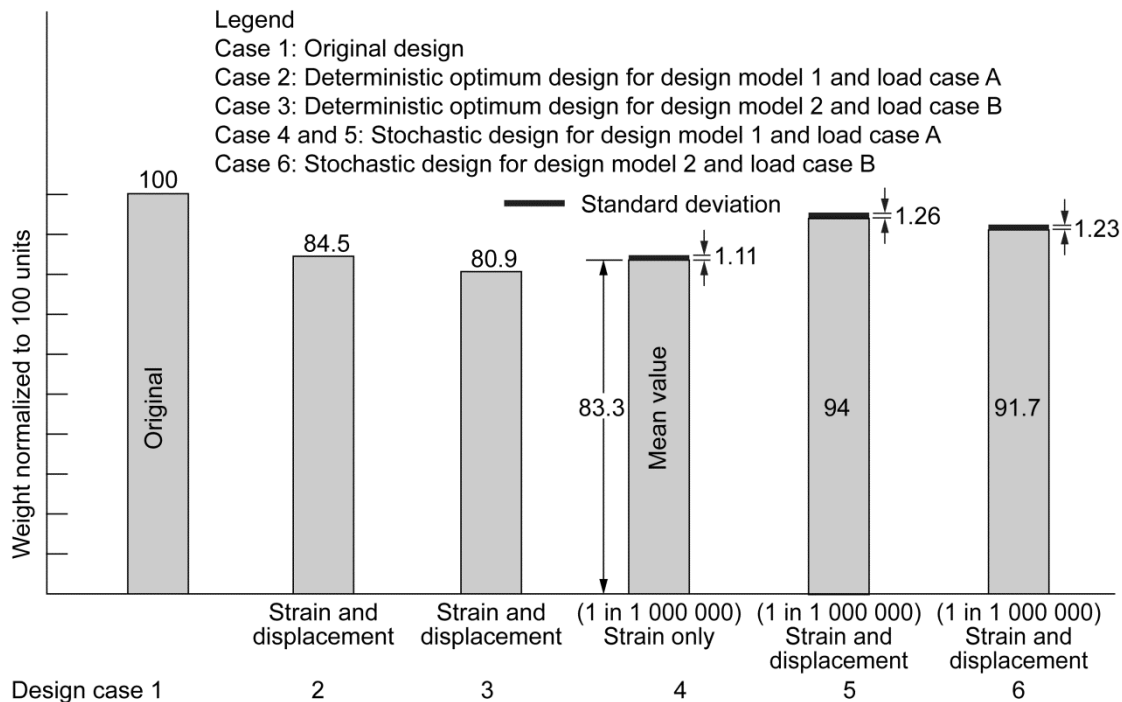


Figure 7.—Optimum weight for six design cases.

The distribution of the strain state in the wingtip was illustrated in Figure 6 for three cases. The first case was the initial design that was supplied by the industry. The second one was the deterministic solution while the third one represented the stochastic design. The strain distribution was uneven for the initial design, and strain exceeds 4000 microstrain at a few localized locations. The distribution of the strain state was more even, for the deterministic and the stochastic design solutions.

Optimum weight for six design cases were depicted the bar chart of Figure 7. The first case with a weight assumed at 100 units represents the original design. All five calculated design cases have lower weight than the original design. The deterministic optimum solution (for strength and stiffness constraints with design model 1 and load case A) generated a 15.5-percent lighter design than the original design. The weight decreased further to 80.9 units when the stiffness constraint was relaxed, see design case 3.

Stochastic optimization produced a mean value for the weight of 83 units with a standard deviation of 1.11 units for strength constraints for design model 1 and load case A for 1 failure in 1,000,000 samples, (see design case 4). The mean value for the weight and a standard deviation increased to 94 and 1.26 units, respectively when stiffness constraint was added to strength limitation, (see design case 5). The mean value of weight and standard deviation reduced to 91.7 and 1.23 units, respectively, for strength and stiffness constraints for design model 2 and load case B (see design case 6 in Fig. 7). Overall, weight can be reduced up to 20 percent depending on the choice of model for design, load, and rate of failure. The standard deviation was small and remained at about 1 percent for the three design cases 4 through 6.

4.2.5 CPU Time to Solution

The CPU time used to reach the solution is given in Table 10. The calculation used CometBoards, which is NASA developed software, along with MSC/Nastran version 2005.5.0 (2005R3) and the FPI module of NESSUS level 6.2 code (1995). Calculations used a Red Hat Linux 2.6.9-67.ELsmp O/S, with x86_64 architecture, 2600 MHz, 4 CPU, 8 GB of memory, and 32-bit numeric format. One static analysis cycle required about 5 CPU seconds. The run time increased to 51 sec for dynamic analysis. Stochastic analysis required about 47 min. Deterministic optimization required about 39 min. The CPU time for stochastic optimization was enormous at 126 to 128 hr of continuous calculations.

TABLE 10.—CPU TIME FOR DESIGN AND ANALYSIS OF WING TIP

Activity	CPU time
One static analysis cycle in MSC/Nastran	5 sec
Dynamic analysis to calculate 20 frequencies in MSC/Nastran	51 sec
Deterministic optimization for design model 1	39 min
Stochastic analysis	47 min
Stochastic optimization: Design model 1 and load model A	128 hr
Stochastic optimization: Design model 2 and load model A	126 hr

Conclusions

The optimization testbed CometBoards with MSC/Nastran and a fast probability integrator successfully generated reliability-based design optimization for an industrial strength raked wing tip structure of a Boeing 767–400 extended range airliner made of metallic and composite materials. The optimization run that required 128 hr or 5.25 days of continuous execution was eventless.

The optimization methodology requires probabilistic models for load, material properties, failure theory, and design parameters. Accuracy of the design solution depends on the models.

Stochastic optimum weight versus reliability produced an inverted-S-shaped plot. Weight increased when risk was reduced and vice versa. The inverted-S graph degenerated into linear segments when a logarithmic scale was used for the x -axis.

The optimization process redistributed the strain field in the structure and achieved up to a 20-percent reduction in weight over the traditional design. The optimum weight was comparable between a deterministic solution and a highly reliable stochastic design. Design of an aircraft structural component must be obtained under multiple load conditions. The maximum strain energy criteria identified a few critical load cases from the many load conditions. The design generated for the critical load was satisfactory. This approach greatly reduced calculation time.

References

1. Guptill, J.D., Hopkins, D.A., Nowden, Terrian V., Pai, S.S., and Patnaik, S.N., “Extension of Optimization Test Bed CometBoards to Probabilistic Design,” 6th Annual FAA/Air Force/NASA/Navy Workshop on the Application of Probabilistic Methods to Gas Turbine Engines, Solomons Island, MD, 2003.

2. Wei, X., "Stochastic Analysis and Optimization of Structures," Ph.D. Dissertation, University of Akron, Akron, OH, 2006.
3. Thacker, B.H., Rhia, D.S., Fitch, S.K., Huyse, L.J., and Pleming, J.B., "Probabilistic Engineering Analysis Using the NESSUS Software, Structural Safety," Vol. 28, No. 1–2, 2006, pp. 83–107.
4. Shinozuka, M., "Monte Carlo Simulation of Structural Dynamics," International Journal for Computers and Structures, Vol. 2, 1972, pp. 855–874.
5. Olson, A.M.J. and Sandberg, G.E., "On Latin Hypercube Sampling for Stochastic Finite Element Analysis", Journal of Engineering Mechanics, 2002, 128(1), pp. 121–125.
6. Guptill, J.D., et al., "CometBoards User Manual Release 1.0.," NASA TM–4537, 1996.
7. Patnaik, S.N., Pai, S.S. and Coroneos, R.M. "Reliability Based Design Optimization of Airframe Components," Proceeding of the Institution of Engineers, Part G, Journal of Aerospace Engineering, Vol. 223, No. 7, 2009, pp. 1019–1036.

REPORT DOCUMENTATION PAGE			Form Approved OMB No. 0704-0188		
<p>The public reporting burden for this collection of information is estimated to average 1 hour per response, including the time for reviewing instructions, searching existing data sources, gathering and maintaining the data needed, and completing and reviewing the collection of information. Send comments regarding this burden estimate or any other aspect of this collection of information, including suggestions for reducing this burden, to Department of Defense, Washington Headquarters Services, Directorate for Information Operations and Reports (0704-0188), 1215 Jefferson Davis Highway, Suite 1204, Arlington, VA 22202-4302. Respondents should be aware that notwithstanding any other provision of law, no person shall be subject to any penalty for failing to comply with a collection of information if it does not display a currently valid OMB control number.</p> <p>PLEASE DO NOT RETURN YOUR FORM TO THE ABOVE ADDRESS.</p>					
1. REPORT DATE (DD-MM-YYYY) 01-11-2011		2. REPORT TYPE Technical Memorandum		3. DATES COVERED (From - To)	
4. TITLE AND SUBTITLE Reliability Based Design for a Raked Wing Tip of an Airframe			5a. CONTRACT NUMBER		
			5b. GRANT NUMBER		
			5c. PROGRAM ELEMENT NUMBER		
6. AUTHOR(S) Patnaik, Surya, N.; Pai, Shantaram, S.; Coroneos, Rula, M.			5d. PROJECT NUMBER		
			5e. TASK NUMBER		
			5f. WORK UNIT NUMBER WBS 561581.02.08.03.13.05		
7. PERFORMING ORGANIZATION NAME(S) AND ADDRESS(ES) National Aeronautics and Space Administration John H. Glenn Research Center at Lewis Field Cleveland, Ohio 44135-3191			8. PERFORMING ORGANIZATION REPORT NUMBER E-17440		
9. SPONSORING/MONITORING AGENCY NAME(S) AND ADDRESS(ES) National Aeronautics and Space Administration Washington, DC 20546-0001			10. SPONSORING/MONITOR'S ACRONYM(S) NASA		
			11. SPONSORING/MONITORING REPORT NUMBER NASA/TM-2011-216808		
12. DISTRIBUTION/AVAILABILITY STATEMENT Unclassified-Unlimited Subject Category: 39 Available electronically at http://www.sti.nasa.gov This publication is available from the NASA Center for AeroSpace Information, 443-757-5802					
13. SUPPLEMENTARY NOTES					
14. ABSTRACT A reliability-based optimization methodology has been developed to design the raked wing tip of the Boeing 767-400 extended range airliner made of composite and metallic materials. Design is formulated for an accepted level of risk or reliability. The design variables, weight and the constraints became functions of reliability. Uncertainties in the load, strength and the material properties, as well as the design variables, were modeled as random parameters with specified distributions, like normal, Weibull or Gumbel functions. The objective function and constraint, or a failure mode, became derived functions of the risk-level. Solution to the problem produced the optimum design with weight, variables and constraints as a function of the risk-level. Optimum weight versus reliability traced out an inverted-S shaped graph. The center of the graph corresponded to a 50 percent probability of success, or one failure in two samples. Under some assumptions, this design would be quite close to the deterministic optimum solution. The weight increased when reliability exceeded 50 percent, and decreased when the reliability was compromised. A design could be selected depending on the level of risk acceptable to a situation. The optimization process achieved up to a 20-percent reduction in weight over traditional design.					
15. SUBJECT TERMS Deterministic; Stochastic; Risk; CometBoards; Distribution; Normal; Weibull; Strain energy; Inverted s-graph; Airframe					
16. SECURITY CLASSIFICATION OF:			17. LIMITATION OF ABSTRACT UU	18. NUMBER OF PAGES 22	19a. NAME OF RESPONSIBLE PERSON STI Help Desk (email:help@sti.nasa.gov)
a. REPORT U	b. ABSTRACT U	c. THIS PAGE U			19b. TELEPHONE NUMBER (include area code) 443-757-5802

